Excitation polarization anisotropy of the spontaneous emission from an *M*-plane GaN film: Competition between hole relaxation and exciton recombination

Oliver Brandt,* Pranob Misra, Timur Flissikowski, and Holger T. Grahn
Paul-Drude-Institut für Festkörperelektronik, Hausvogteiplatz 5–7, 10117 Berlin, Germany
(Received 6 December 2012; revised manuscript received 26 February 2013; published 29 April 2013)

We investigate a strongly anisotropically strained *M*-plane GaN film by photoluminescence spectroscopy. The spectra are dominated by the lowest-energy free-exciton transition, but the second lowest one is also detectable even at low temperatures. Rotating the linear polarization of the excitation results in a systematic change of the intensity ratio between these two transitions. We analyze this observation with the help of 6×6 $\mathbf{k} \cdot \mathbf{p}$ calculations and associated rate equation models. This analysis shows that the pronounced excitation polarization anisotropy for this *M*-plane GaN film originates from a competition between hole relaxation and exciton recombination.

DOI: 10.1103/PhysRevB.87.165308 PACS number(s): 73.50.Gr, 78.55.Cr, 78.47.J−, 78.20.Bh

The spontaneous emission of semiconductors is frequently excited with an energy in excess of the semiconductor's band gap. In a polar semiconductor such as GaAs or GaN, this excess energy may be rapidly released by the emission of longitudinal optical (LO) phonons within a time of about 200 fs.[1,2] In contrast, the spontaneous emission in these compounds takes place on a time scale of several ns to μs (depending on temperature)[3–6] and thus occurs by the recombination of completely thermalized electrons and holes. For this reason, the resulting luminescence spectrum bears neither any information about its excitation and the subsequent relaxation of carriers prior to their recombination (with the notable exception of hot electron luminescence in doped semiconductors),[7,8] nor is it influenced by the properties of the electronic bands at the point of excitation. Consequently, investigations of the ultrafast initial carrier dynamics generally require pump-probe or luminescence up-conversion techniques with sub-ps time resolution.[9–13]

The compound semiconductor GaN preferentially crystallizes in the wurtzite structure and thus inherently exhibits a uniaxial optical anisotropy.[14] This peculiarity manifests itself primarily in a linear birefringence in the transparent spectral range and a linear dichroism in the absorptive spectral range of these materials.[15,16] These properties may be readily accessed for group-III nitride thin films oriented such that the *c* axis lies in-plane, as it is the case for $[11\bar{2}0]$ (*A*-plane) or $[10\bar{1}0]$ (*M*-plane) epitaxial films. Because absorption and emission are fundamentally linked,[17] the spontaneous emission of these epitaxial films is polarized as well.[18–23] Anisotropic in-plane strain may split the uppermost valence bands to such a degree that this emission polarization remains high even at room temperature.[24]

In this paper, we investigate a highly strained *M*-plane GaN film by polarization-resolved photoluminescence (PL) spectroscopy. The ground-state exciton emission from this film is strongly polarized with a polarization degree of 87% at room temperature. The exciton emission associated with the next-highest valence band can be detected even at temperatures as low as 20 K despite the fact that it occurs at a 50 meV higher energy. To understand this phenomenon, we investigate our *M*-plane GaN film by polarization-dependent PL spectroscopy, i.e., we systematically tune the excitation polarization while recording the PL spectra of the film. The intensity ratio between the two lowest exciton transitions is found to mimic the polarization of the bands at the point of excitation. This polarization memory reflects a nonthermalized carrier distribution, which originates from the similar magnitude of the exciton lifetime and the relaxation time of holes.

The *M*-plane GaN film under investigation was grown by radio-frequency plasma-assisted molecular-beam epitaxy on a γ-$LiAlO_2(100)$ substrate.[25] The particular plasma source used for growth (a first generation model from SVT Associates Inc.) is known to produce high-energy ions inducing significant radiation damage and thus high concentrations of point defects. These defects act as both compensating traps and nonradiative recombination centers, resulting in highly resistive films with short carrier lifetime considered to be of interest for fast optical modulators and polarization filters.[26] The thickness of the film under investigation (700 nm) was kept sufficiently low to sustain its highly strained state and thus to ensure a large energy splitting between the two lowest exciton transitions. Triple-axis x-ray diffraction scans show the film to be under an overall compressive in-plane strain with an exceptionally large out-of-plane dilation of $\varepsilon_{yy} = 0.45\%$. These measurements do not provide information on the in-plane strain, which is inevitably anisotropic ($\varepsilon_{xx} \neq \varepsilon_{zz}$) due to the anisotropic lattice and thermal mismatch between $GaN(10\bar{1}0)$ and γ-$LiAlO_2(100)$.

Continuous-wave PL spectroscopy is carried out using a confocal micro-PL setup equipped with a Cryovac microscope cryostat facilitating measurements between 10 and 300 K. For excitation, we use the 325 nm (3.815 eV) line of a Kimmon He-Cd laser attenuated by reflective filters and focused to a micrometer-sized spot by a 15× microscope objective. The resulting excitation density on the sample is about 1 kW/cm^2. The polarization of the laser is controlled by a double Fresnel rhomb, and the polarization of the PL emitted from the sample is analyzed by a half-wave plate and a Glan-Taylor prism. Measurements of the total PL intensity are achieved with the help of a quarter-wave plate which effectively depolarizes the emission. The PL signal passing either the analyzer or the depolarizer is spectrally dispersed by a 0.8 m Jobin-Yvon monochromator and detected with a cooled charge-coupled-device detector.

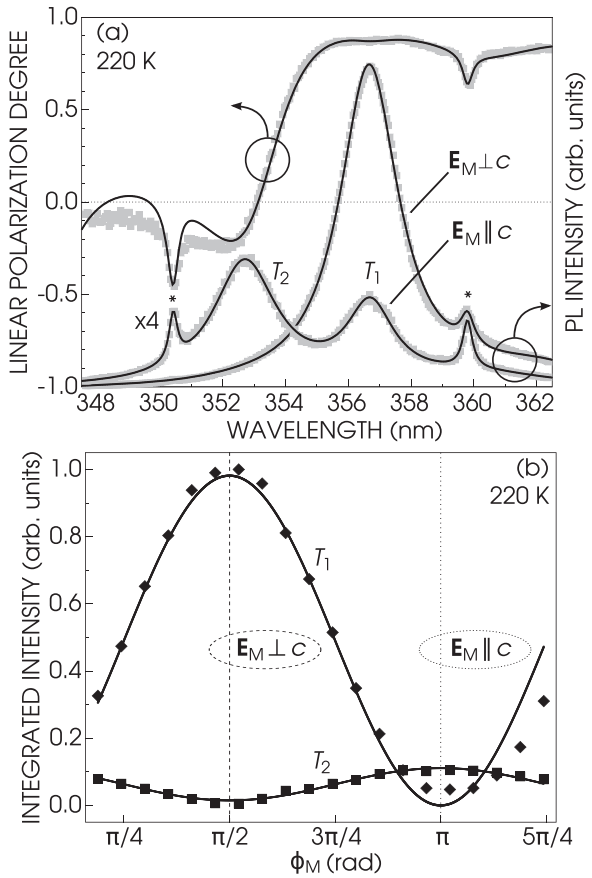

FIG. 1. (a) Polarized PL spectra and spectrally resolved linear PL polarization of the M-plane GaN film under investigation at 220 K. The spectra are recorded by detecting the emission with an analyzer set to pass only light with an electric field $\mathbf{E}_M$ parallel or perpendicular to the c axis of the film. The two PL lines observed originate from the two lowest exciton transitions in the anisotropically strained M-plane GaN film and are designated as T_1 and T_2. The sharp peaks labeled with an asterisk originate from third and fourth order resonant Raman scattering. Symbols denote the measurements and solid lines a line-shape fit used to determine the spectrally integrated intensities of T_1 and T_2. The dotted line indicates the position of zero polarization. (b) Spectrally integrated intensity of the two PL lines T_1 and T_2 at 220 K as a function of the analyzer angle ϕ_M. Symbols indicate experimental results, and the solid line is a fit showing that the data obey Malus' law (Ref. 27). The dashed and dotted lines highlight the analyzer angles for which $\mathbf{E}_M \perp c$ and $\mathbf{E}_M \parallel c$, respectively.

We first characterize the basic properties of the M-plane GaN film under investigation using polarized PL spectroscopy. Figure 1(a) shows the polarized PL spectra of this film at 220 K. We have chosen this elevated temperature since the large valence-band splitting of M-plane GaN films facilitates the observation of the higher exciton transition T_2. At the same time, we expect the thermal broadening of the transitions of about 20 meV to be still sufficiently low to spectrally separate the two lowest exciton transitions T_1 and T_2 in the anisotropically strained M-plane GaN film. Indeed, these transitions manifest themselves as well-resolved lines at 356.7 and 352.7 nm (3.475 and 3.514 eV) in the spectra displayed in Fig. 1(a). The energy splitting of 39 meV between these two transitions as well as the 40 meV blueshift of the T_1 transition with respect to the expected position for unstrained material reflect the magnitude of the elastic strain in the film. In-plane strain components of $\varepsilon_{xx} = -0.88$ and $\varepsilon_{zz} = -0.46\%$ are obtained by diagonalizing the 6×6 Bir-Pikus $\mathbf{k} \cdot \mathbf{p}$ Hamiltonian as a function of the in-plane strain components[24] and comparing the resulting transition energies for $\mathbf{k} = 0$ to the spectral positions of the T_1 and T_2 transitions observed experimentally.[28]

The degree of the linear polarization of the PL spectra is defined as $(I_\perp - I_\parallel)/(I_\perp + I_\parallel)$. The resulting spectrally resolved polarization degree is also shown in Fig. 1(a). The T_1 transition exhibits a polarization degree of 87%, while it appears to be only -25% for the T_2 transition. This low polarization degree arises from the significant thermal broadening of the transitions at this elevated temperature. At low temperatures (not shown here), both transitions exhibit a polarization degree of more than 90% as expected theoretically.

For obtaining the spectrally integrated intensity of the T_1 and T_2 transitions, four Lorentzians are fit to the experimental data. Figure 1(b) shows the results of these fits as a function of the analyzer angle ϕ_M. The lines represent fits of Malus' law[27] for the intensity $I(\phi_M) = I_\perp \cos^2(\phi_M) + I_\parallel \sin^2(\phi_M)$ to the data. Evidently, the polarization of both transitions is well described by two orthogonal components parallel and perpendicular to c. In fact, transition T_1 is purely x polarized since $I_\parallel$ is essentially zero. For T_2, $I_\perp/I_\parallel \approx 0.1$, making this transition predominantly z polarized. These results are in excellent agreement with the oscillator strengths obtained from our $\mathbf{k} \cdot \mathbf{p}$ calculations at $\mathbf{k} = 0$.

We now discuss experiments in which the excitation polarization was changed in a controlled way. Figures 2(a) and 2(b) display the polarized PL spectra of the M-plane GaN

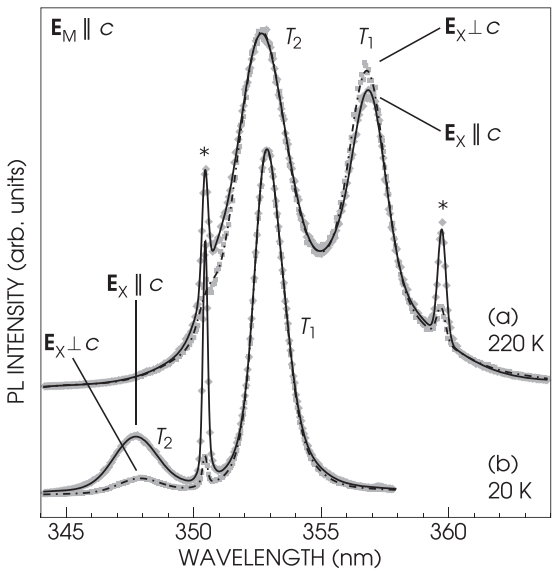

FIG. 2. Polarized PL spectra of the M-plane GaN film excited by linearly polarized light with the electric field $\mathbf{E}_X$ parallel (diamonds and solid line) and perpendicular (squares and dash-dotted line) to the c axis of the film, and detected with $\mathbf{E}_M \parallel c$. (a) Spectra recorded at 220 K and normalized to the peak intensity of the T_2 transition. (b) Spectra recorded at 20 K and normalized to the peak intensity of the T_1 transition.

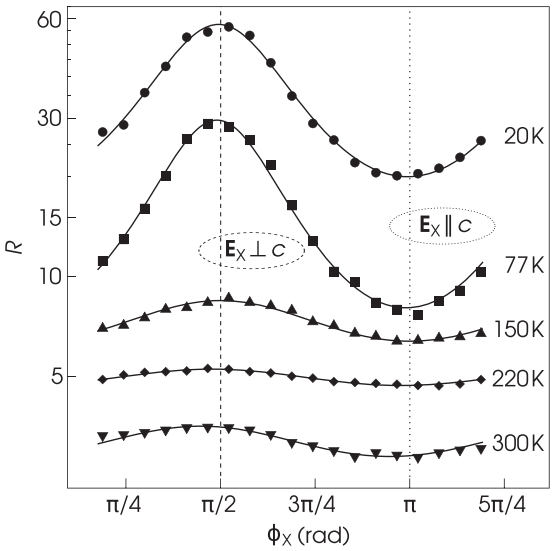

FIG. 3. Ratio of the spectrally integrated total intensity of the two PL lines T_1 and T_2 as a function of the polarizer angle ϕ_X for various temperatures. The emission is detected depolarized. Symbols indicate experimental results, and the solid line is a fit with the rate-equation model described in the text.

film at 220 and 20 K, respectively. The spectra were excited by linearly polarized light with the electric field $\mathbf{E}_X$ parallel and perpendicular to the c axis of the film, and detected with $\mathbf{E}_M \parallel c$. Clearly, the intensity ratio of the T_1 and T_2 transitions depends on the polarization of the excitation. The change of the intensity ratio with excitation polarization is more pronounced at 20 than at 220 K. The sharp peaks arising from higher-order resonant Raman scattering exhibit an ever stronger dependence on polarization, but that is to be expected: The higher-order $A_1(LO)$ excitations are allowed only in polarized, i.e., here the $y(z,z)\bar{y}$, configuration, just as experimentally observed. For a PL transition excited high in the band, however, this observation is unexpected since the photogenerated holes, once having relaxed all excess energy and occupying the minimum of valence band V_1 near $\mathbf{k} = 0$, should not retain a memory of their point of excitation.

Figure 3 shows the ratio R of the spectrally integrated, total intensity (i. e., measured with depolarized detection) of the two PL lines T_1 and T_2 as a function of the polarizer angle ϕ_X for temperatures between 20 and 300 K. The angular dependence of R resembles the polarization of the emission itself as shown in Fig. 1(b). The polarization of R, defined as $(R_\perp - R_\parallel)/(R_\perp + R_\parallel)$, is highest at 77 and lowest at 220 K. The average value of R increases monotonically with decreasing temperature, but much less than expected when considering the purely thermal occupation of the bands. At 20 K, for example, $k_B T = 1.7$ meV, while the splitting of the V_1 and V_2 bands amounts to 57.3 meV as determined from the spectral positions of the corresponding PL transitions T_1 and T_2, respectively [cf. Fig. 2(b)]. The photoexcited holes are thus far from being thermalized in these experiments.

To develop an understanding of this excitation polarization anisotropy, we examine the valence band dispersion at 220 K and finite values of $\mathbf{k}$. Note that the simple Bir-Pikus model used is *not* quantitatively reliable for large values of $\mathbf{k}$[29,30]

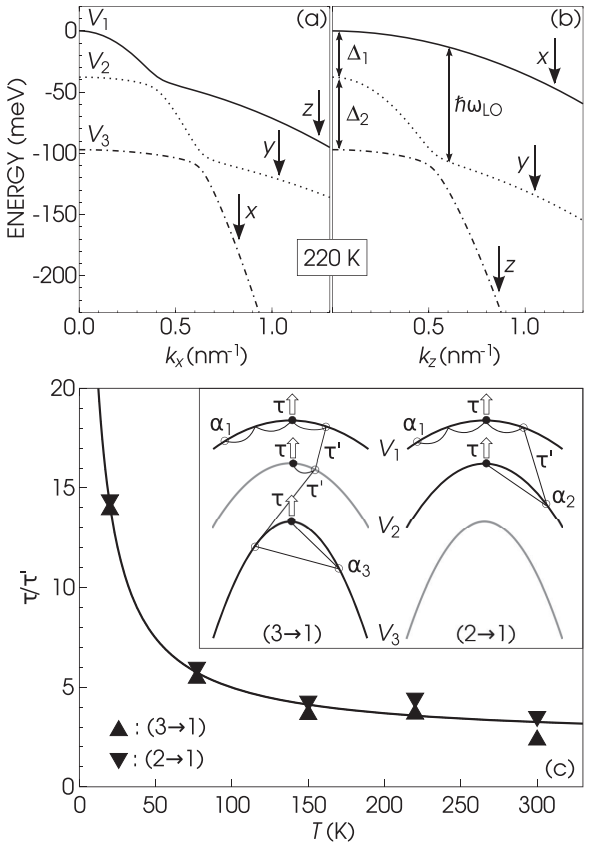

FIG. 4. Dispersion of the upper three valence bands V_i ($i = 1 \ldots 3$) of GaN along (a) k_x and (b) k_z calculated within the frame of a Bir-Pikus $\mathbf{k} \cdot \mathbf{p}$ approach for in-plane strain components determined from the spectral positions of the transitions T_1 and T_2 at 220 K. The energy splittings of the bands at $\mathbf{k} = \mathbf{0}$ are denoted as Δ_1 and Δ_2. The downward arrows indicate the $\mathbf{k}$ values at which excitation with an energy of 3.815 eV occurs. The energy difference between these values reflects the dispersion of the conduction band (not shown). The LO phonon energy $\hbar\omega_{LO}$ is shown as a natural energy scale. (c) Ratio of the exciton lifetime τ and relaxation time τ' as a function of temperature as deduced from fits to the experimental data [cf. Fig. 3]. The line is a guide to the eye, and the up- and downward triangles denote the results of the fits using the two different models depicted in the inset and defined in the text. Excitation within a specific band V_i is indicated with α_i. The photoexcited holes may subsequently relax within this band toward $\mathbf{k} = 0$ and recombine, or scatter into a lower band.

and should rather be seen as a qualitative guide. As shown in Figs. 4(a) and 4(b), anticrossings occur between the bands, which change their character depending on the direction in $\mathbf{k}$ space. Regardless of these anticrossings, the bands are predicted to retain a purely linearly polarized character at high values of $\mathbf{k}$. For example, the predicted predominant symmetry of the V_1, V_2, and V_3 bands is z, y, and x, respectively, at the values of k_x corresponding to the points of excitation [downward arrows in Fig. 4(a)]. It is thus easily understandable that the photoexcitation of holes depends on the polarization of the incident light. Specifically, for z polarized excitation (i.e., for $\mathbf{E}_X \parallel c$ and thus $\phi_X = \pi$), holes would be generated predominantly in V_1 along k_x [Fig. 4(a)], but in V_3 along k_z [Fig. 4(b)]. These photoexcited holes will initially relax their

excess energy within a sub-ps time scale by the emission of LO phonons [see the corresponding scale bar in Fig. 4(b)], and subsequently by acoustic phonons near the bottom of the bands.

According to the calculated dispersion shown in Figs. 4(a) and 4(b), the valence band V_2 exhibits y symmetry at the energy of excitation independent of the direction of $\mathbf{k}$. The dipole matrix elements for transitions involving V_2 are thus zero for x and z polarized light, and holes can be excited only for valence bands V_1 and V_3. A simple rate-equation model describing the relaxation-recombination dynamics for this case [thereafter denoted as $3 \rightarrow 1$, and illustrated in the inset of Fig. 4(c)] is represented by the following linear algebraic equations:

$$\frac{dp_1}{dt} = \alpha_1 G - \frac{p_1}{\tau} + \frac{p_2}{\tau'} - \frac{p_1}{\tau_b'} = 0 \quad (1)$$

$$\frac{dp_2}{dt} = -\frac{p_2}{\tau} - \frac{p_2}{\tau'} + \frac{p_1}{\tau_b'} + \frac{p_3}{\tau'} = 0 \quad (2)$$

$$\frac{dp_3}{dt} = \alpha_3 G - \frac{p_3}{\tau} - \frac{p_3}{\tau'} = 0. \quad (3)$$

Excitation of holes occurs with the total generation rate G. The dimensionless prefactors $\alpha_i(\phi_X)$ ($\sum_i \alpha_i = 1$) account for the fraction of holes p_i generated in the valence bands V_i according to their normalized oscillator strength for the given energy and polarization. For each band, the oscillator strength is proportional to the dipole matrix elements integrated over all values of $\mathbf{k}$ for which $E(\mathbf{k}) = 3.815$ eV. After excitation, all holes are supposed to relax within their band instantaneously, scatter to a lower band within the time τ', form excitons with electrons instantaneously, and recombine thereafter with an effective lifetime τ comprising both radiative and nonradiative contributions. The integrated intensity of the experimentally observed transitions T_1 and T_2 is given by p_1/τ_r and p_2/τ_r, respectively, with the radiative lifetime τ_r. Note the simplifying assumptions that all relaxation and recombination times are equal, and the neglect of a direct interaction between V_1 and V_3. Thermal redistribution of holes across V_1 and V_2 is taken into account by $\tau_b' = \tau' \exp(\Delta_1/k_B T)$, but is neglected across V_2 and V_3 as well as V_1 and V_3 since $\Delta_2 > \Delta_1$ [with Δ_1 and Δ_2 denoting the energy splittings of the bands at $\mathbf{k} = \mathbf{0}$ as depicted in Fig. 4(b)]. In the limit of $\tau \gg \tau'$, the solution of the Eqs. (1)–(3) approaches the result expected for fully thermalized holes, i.e., $p_2/p_1 = \exp(-\Delta_1/k_B T)$. In this case, the PL intensity ratio R would be a constant independent of the polarization angle ϕ_X. The angular variation of R observed in our experiments (cf. Fig. 3) as well as its small value particularly at low temperatures reveal that τ and τ' have to be of similar magnitude for the sample under consideration.

Since the simple Bir-Pikus model used for calculating the valence band dispersion may not predict the correct valence band symmetry for large values of $\mathbf{k}$, the above assumption of $\alpha_2 = 0$ may be incorrect as well. In reality, holes may be generated in all three valence bands to a varying degree, and relaxation as well as recombination within and from all bands would occur. A corresponding rate-equation model is straightforward to formulate and to solve, but contains too many parameters for a unique fit to the experimental data. Instead of permitting the excitation of holes in all valence bands, we thus consider the *opposite* case to the above approximate model $3 \rightarrow 1$ in that we assume that valence band V_3 cannot be excited [model $2 \rightarrow 1$ in the inset of Fig. 4(c)]:

$$\frac{dp_1}{dt} = \alpha_1 G - \frac{p_1}{\tau} + \frac{p_2}{\tau'} - \frac{p_1}{\tau_b'} = 0 \quad (4)$$

$$\frac{dp_2}{dt} = \alpha_2 G - \frac{p_2}{\tau} - \frac{p_2}{\tau'} + \frac{p_1}{\tau_b'} = 0. \quad (5)$$

Once again, $p_2/p_1 = \exp(-\Delta_1/k_B T)$ for $\tau \gg \tau'$.

Equations (1)–(3) and (4) & (5) can both be solved easily for arbitrary τ and τ', and we can thus fit the corresponding PL intensity ratio R with the respective ratio p_1/p_2 (since we assume equal radiative lifetimes). To reduce the number of free parameters, we set $\alpha = \alpha_1 = 1 - \alpha_2 = 1 - \alpha_3$. Furthermore, we suppose that the polarization dependence contained in the prefactor α may be expressed as expected from an examination of Figs. 4(a) and 4(b), namely, $\alpha = \alpha_\perp \cos^2(\phi_X) + \alpha_\parallel \sin^2(\phi_X)$. We computed α within the frame of our 6×6 $\mathbf{k} \cdot \mathbf{p}$ Hamiltonian and found a dependence much resembling this simple form, and even with an anisotropy decreasing with temperature in agreement with experiment. We still doubt, however, that the values derived are quantitatively meaningful, and we thus treat both $\alpha_\perp$ and $\alpha_\parallel$ as well as the ratio of the recombination and relaxation times τ/τ' as free parameters in our further analysis. The resulting best fits are depicted as solid lines in Fig. 3. The two models yield fits indistinguishable from each other and also deliver very similar values for the free parameters. This observation holds in particular for the lifetime ratio τ/τ', which is plotted in Fig. 4 as obtained from the fits vs temperature.

Evidently, the value of this ratio does not critically depend on the nature of the bands participating in recombination. In fact, τ/τ' is determined primarily by the absolute magnitude of the experimentally obtained intensity ratio and much less by its modulation. Hence, the values derived for this ratio are meaningful independent of our assumptions regarding the prefactor α. The apparent polarization memory of excitons can thus be explained simply by their inability to thermalize due to the fact that their relaxation and recombination occurs on essentially equal time scales. Note that it is the purely linearly polarized character of the bands which actually facilitates the detection of this effect as well as its quantitative analysis.

If we could obtain absolute values for τ by independent means, we should be able to determine the hole relaxation time. Consequently, we have attempted to measure τ by exciting the sample by fs laser pulses and analyzing the transient PL signal with a streak camera. The decay times thus obtained, however, were too close to the time resolution of the setup, and we can only state with certainty that, independent of temperature, $\tau < (6 \pm 2)$ ps for the T_1 and $\tau < (4 \pm 2)$ ps for the T_2 transition. The difference in these times directly indicates that the relaxation of holes takes place within approximately 1–2 ps. Comparing the measured lifetimes with Fig. 4(c) confirms this value, which is also in agreement with the one derived from pump-probe experiments.[31]

Much more accurate values would be obtained, of course, for samples with slightly longer recombination lifetimes. Such samples could be produced intentionally by ion implantation of high-quality M-plane GaN films with a systematically varying irradiation dose. Measurements analogous to those presented

here would then enable us to measure the hole relaxation time as a function of various parameters such as, for example, the doping level. With a tunable laser as excitation source, we could simultaneously obtain the dipole matrix elements as a function of both in-plane polarization and energy E, thus enabling us to map the electronic band structure of the film. In either case, the measurements could be performed by utilizing standard cw and ps photoluminescence techniques without the need for sophisticated femtosecond pump-probe or up-conversion setups.

We thank Vladimir M. Kaganer for providing a robust and fast batch fitting routine, Sandip Ghosh (Tata Institute of Fundamental Research) for encouragement and support, and Manfred Ramsteiner for a critical reading of the manuscript.

*brandt@pdi-berlin.de

[1] J. A. Kash, J. C. Tsang, and J. M. Hvam, Phys. Rev. Lett. **54**, 2151 (1985).
[2] H. Ye, G. Wicks, and P. Fauchet, Appl. Phys. Lett **74**, 711 (1999).
[3] G. W.'t Hooft, W. A. J. A. van der Poel, L. W. Molenkamp, and C. T. Foxon, Phys. Rev. B **35**, 8281 (1987).
[4] P. Asbeck, J. Appl. Phys. **48**, 820 (1977).
[5] O. Brandt, J. Ringling, K. H. Ploog, H.-J. Wünsche, and F. Henneberger, Phys. Rev. B **58**, R15977 (1998).
[6] P. Ŝĉajev, K. Jaraŝiūnas, S. Okur, U. Özgür, and H. Morkoç, J. Appl. Phys. **111**, 023702 (2012).
[7] G. Fasol, W. Hackenberg, H. P. Hughes, K. Ploog, E. Bauser, and H. Kano, Phys. Rev. B **41**, 1461 (1990).
[8] V. F. Sapega, M. Ramsteiner, O. Brandt, L. Däweritz, and K. H. Ploog, Phys. Rev. B **73**, 235208 (2006).
[9] C. J. Stanton, D. W. Bailey, and K. Hess, Phys. Rev. Lett. **65**, 231 (1990).
[10] T. Elsaesser, J. Shah, L. Rota, and P. Lugli, Phys. Rev. Lett. **66**, 1757 (1991).
[11] D. W. Snoke, W. W. Rühle, Y.-C. Lu, and E. Bauser, Phys. Rev. Lett. **68**, 990 (1992).
[12] L. Rota, P. Lugli, T. Elsaesser, and J. Shah, Phys. Rev. B **47**, 4226 (1993).
[13] D. J. Hilton and C. L. Tang, Phys. Rev. Lett. **89**, 146601 (2002).
[14] P. Misra, O. Brandt, H. T. Grahn, H. Teisseyre, M. Siekacz, C. Skierbiszewski, and B. Łucznik, Appl. Phys. Lett. **91**, 141903 (2007).
[15] P. Misra, Y. J. Sun, O. Brandt, and H. T. Grahn, J. Appl. Phys. **96**, 7029 (2004).
[16] D. M. Schaadt, O. Brandt, S. Ghosh, T. Flissikowski, U. Jahn, and H. T. Grahn, Appl. Phys. Lett. **90**, 231117 (2007).
[17] W. van Roosbroeck and W. Shockley, Phys. Rev. **94**, 1558(1954).
[18] B. Rau, P. Waltereit, O. Brandt, M. Ramsteiner, K. H. Ploog, J. Puls, and F. Henneberger, Appl. Phys. Lett. **77**, 3343 (2000).
[19] Y. J. Sun, O. Brandt, B. Jenichen, and K. H. Ploog, Appl. Phys. Lett. **83**, 5178 (2003).
[20] N. Gardner, J. Kim, J. Wierer, Y. Shen, and M. Krames, Appl. Phys. Lett. **86**, 111101 (2005).
[21] T. Koyama, T. Onuma, H. Masui, A. Chakraborty, B. Haskell, S. Keller, U. Mishra, J. Speck, S. Nakamura, S. DenBaars *et al.*, Appl. Phys. Lett. **89**, 091906 (2006).
[22] C. Rivera, P. Misra, J. L. Pau, E. Muñ, O. Brandt, H. T. Grahn, and K. H. Ploog, J. Appl. Phys. **101**, 053527 (2007).
[23] M. Schubert, S. Chhajed, J. Kim, E. Schubert, and J. Cho, Appl. Phys. Lett. **91**, 051117 (2007).
[24] S. Ghosh, P. Waltereit, O. Brandt, H. T. Grahn, and K. H. Ploog, Phys. Rev. B **65**, 075202 (2002).
[25] O. Brandt, Y. J. Sun, L. Däweritz, and K. H. Ploog, Phys. Rev. B **69**, 165326 (2004).
[26] K. Omae, T. Flissikowski, P. Misra, O. Brandt, H. T. Grahn, K. Kojima, and Y. Kawakami, Appl. Phys. Lett. **86**, 191909 (2005).
[27] J. Buchwald, *The Rise of the Wave Theory of Light: Optical Theory and Experiment in the Early Nineteenth Century* (University of Chicago Press, Chicago and London, 1989).
[28] P. Misra, U. Behn, O. Brandt, H. T. Grahn, B. Imer, S. Nakamura, S. P. DenBaars, and J. S. Speck, Appl. Phys. Lett. **88**, 161920 (2006).
[29] R. Beresford, J. Appl. Phys. **95**, 6216 (2004).
[30] A. Marnetto, M. Penna, and M. Goano, J. Appl. Phys. **108**, 033701 (2010).
[31] T. Flissikowski, K. Omae, P. Misra, O. Brandt, and H. T. Grahn, Phys. Rev. B **74**, 085323 (2006).